Demonstration of high-speed data transmission using MIMO-OFDM visible light communications

Ahmad Helmi Azhar and Tuan-Anh Tran, Dominic O'Brien *Member IEEE.*

***Abstract*—This letter reports an experimental demonstration of high-speed indoor optical wireless Optical multiple-input multiple-output (MIMO)-orthogonal frequency division multiplexing (OFDM) system with an imaging receiver. The system consists of a 2x1 array of white LEDs that transmit data to a 9 channel imaging receiver that uses a 3x3 photodetector array. A total transmission rate of 220Mbit/s at a BER of 10^{-3} is achieved over a range of 1m.**

An overview of the design specifications, optical design and experimental setup are reported in this letter, together with results and discussion of how improvements to the system may be achieved.

***Index Terms*—Imaging MIMO, OFDM, MIMO-OFDM, MIMO systems, Visible light communications**

I. INTRODUCTION

SOLID state lighting typically uses arrays of white-light LEDs to generate the required level of illumination for the particular system concerned. These devices can be used for communications as well as illumination and visible light communication (VLC) is an area of growing interest[1] with a forthcoming IEEE standard[2]. However, the bandwidth of these sources are limited and schemes such as equalisation [3] and complex modulation [4] can be used to increase data rates.

Orthogonal frequency division multiplexing (OFDM) has found favour for VLC [5, 6] because of the high SNR [4] low bandwidth [3] channel that is characteristic of typical white-Light LED based systems. Recently VLC transmission at 231Mbps using OFDM has been reported [23].

Imaging [7] and angle diversity [8] transmitters and receivers can be used in various Multiple-Input-Multiple-Output (MIMO) configurations in indoor environments and there have been a number of investigations and demonstrations in this area (see for instance[9-14]). There is also similar work in the area of optical interconnection for computing systems (see[15] for a review). The optimal MIMO configuration would be to align an array of sources with an array of detectors, forming distinct parallel channels with no crosstalk between them.

A. H. Azhar, T.-A. Tran and D. C. O'Brien are with the Department of Engineering Science, University of Oxford, Oxford OX1 3PJ, UK (e-mail: dominic.obrien@eng.ox.ac.uk).

However, this alignment is difficult to achieve with terminal mobility, and MIMO processing removes the need for precise mechanical alignment, effectively moving alignment to the electronic domain. In [16], a demonstration of a 4x9 imaging line of sight optical multiple-input multiple-output (MIMO) system is detailed. This system transmits On-Off Keying (OOK) data at 2Mbps/channel. In this paper we report a system that carries OFDM coded data in a 2x9 MIMO system, using the same imaging receiver as that reported in [16]. The paper is organised as follows; the demonstrator and experimental setup are described in Section II. Section III explains the signal processing and the experimental results are presented in Section IV. Finally, discussions are presented and conclusions are drawn in Section V.

II. SYSTEM DESCRIPTION

A. System Overview

Fig. 1 shows the system. A stream of random binary data is generated in software (MATLAB) and this is split into two parallel streams, each of which is passed to a software-based OFDM encoder, one for each transmitter (Tx) channel. The resulting OFDM waveforms are then loaded into an arbitrary-waveform generator. The output of this generator is combined with a DC-bias current using a bias-T and the resulting waveform is applied to a white LED acting as an optical transmitter.

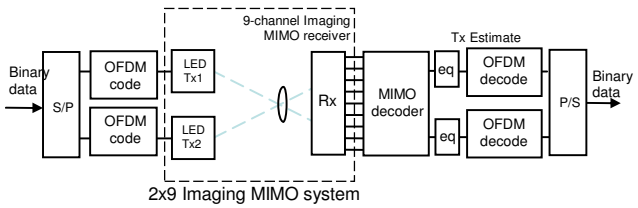

Fig. 1. MIMO-OFDM system block diagram.

Light from the LEDs propagates to a 9-channel imaging optical receiver (Rx)[7]. The received signals from each of the 9 channels are routed to an oscilloscope and are acquired and transferred to a control computer for subsequent processing. Details of the particular receiver can be found in [17]. The

received data streams are processed in a MIMO demultiplexer to recover an estimate of the two transmitted signals. Then, since the white LEDs used as transmitters have a limited bandwidth, each of the two signals are independently post-equalised [3]. The equalised streams are then passed through the OFDM decoder to recover the original binary stream.

B. Data Generation and Transmission

The binary data stream is modulated into a set of sub-carrier symbols using a 4-quadrature amplitude modulation scheme (4-QAM). The demonstrator uses a 64-point Inverse Fast Fourier Transform (IFFT) to construct a frame of 64-OFDM symbols. This is done by assigning the set of sub-carrier symbols into equally spaced slots in the frequency domain across the transmission bandwidth.

The frequency band is divided into 2 bins. The first symbol of each bin is assigned a zero to ensure symmetrical IFFT transformation. The 31 slots of active data sub-carriers in the first bin are matched with their own Hermitian conjugates, which are loaded into the second bin. This Hermitian matching is required for an all-real output (i.e. no imaginary component) from the IFFT algorithm [6].

C. Link Budget

In IM/DD, optical power collected at the photodiode is converted to electrical current. The output current, i, is given by

$$i = P_{rx} * R, \tag{1}$$

where R is the photodiode responsivity (A/W) and P_{rx} is the received optical power.

The signal-to-noise ratio (SNR) is given by

$$SNR = \frac{i^2}{\sigma^2}, \tag{2}$$

where σ^2 is the total noise variance. This is the summation of the shot noise variance, σ^2_{shot} and the amplifier noise variance, σ^2_{amp} and is given by

$$\sigma^2 = \sigma^2_{shot} + \sigma^2_{amp}. \tag{3}$$

The shot noise variance is given by

$$\sigma^2_{shot} = 2qRP_{rx}B_n, \tag{4}$$

where q is the electron charge, P_n is the background noise power, and B_n is the noise bandwidth, which is taken to be the same as receiver bandwidth, B. The amplifier noise variance, σ^2_{amp} is given by

$$\sigma^2_{amp} = N^2_{amp}B_n, \tag{5}$$

where N_{amp} is the amplifier noise density.

The illuminance [lux, lx], E is given by

$$E = \frac{\Phi}{A}, \tag{6}$$

where Φ is luminous flux [lumen, lm], and A is the collection area of the receiver lens. The incident power can be estimated by converting from lumens to watts, and for this representative result from the literature (4.2mW/lm[4]) is used. Table 1 shows the other calculation parameters. The minimum estimated SNR is ~88dB at 400 lux (a level acceptable for room illumination) for a 2MHz bandwidth channel (corresponding to the LED bandwidth), which is much higher than the required SNR to achieve the target BER.

The modulation experiments use carriers up to 70MHz, and for a flat channel not limited by the LED frequency response the increased noise bandwidth would lead to an estimated SNR of 71dB. However, as can be seen from the channel response in Fig. 2 there is an ~30dB-40dB drop in modulated power at 70 MHz compared with low frequency, leading to an estimated SNR of ~30-40dB. These indicate that the system is not limited by SNR, and are in broad agreement with results from others[4].

Table 1. Link budget calculation parameters.

Parameter	Description
Receiver responsivity, R	0.4A/W (white)
Noise power density, N_{amp}	5pA/√Hz
Illuminance, E	400lx
Collection area A	5.1cm^2

D. Experimental Setup

Fig. 2 shows the experimental set-up for the MIMO-OFDM demonstrator and Fig. 3 shows photographs of the transmitter and receiver components. The transmitter consists of 2 Luxeon Star white LEDs separated by a distance s. Each LED is fitted with a diffusing lens with half-angle, $\theta = 5^\circ$.

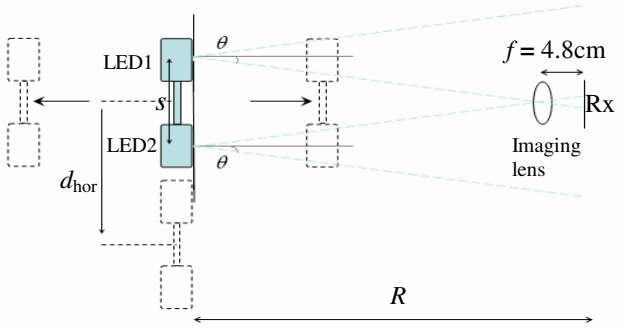

Fig. 2. Plan view of the set-up for both range and coverage area of the 3x3 detector system. Variable d_{hor} denotes the linear coverage on the horizontal direction.

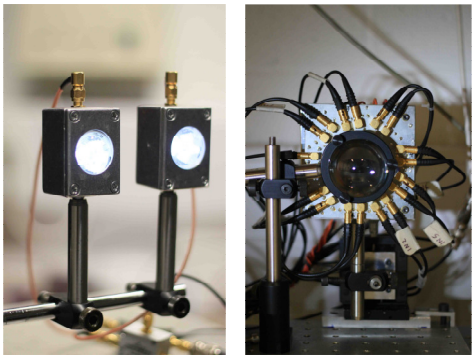

Fig. 3 Transmitter array with 2 LEDs with diffusing lenses (left) and Imaging receiver setup (right).

The 3x3 photo-detector array used in the imaging receiver has an individual pixel size of 2.7mm with 0.1mm separation. The receiver is fitted with an imaging lens with a focal length f = 4.8cm and f-number of 1. Apart from focusing the beams onto the photo-detectors, the lens acts as an optical collector to ensure a high proportion of light is captured.

The arbitrary waveform generator output voltage is set at a level where there is sufficient modulation to saturate the imaging receiver, resulting some signal clipping for low frequency components. This reduces the BER compared to cases without clipping (in common with other results [18, 19]).

III. Signal Processing for OFDM-MIMO VLC

A. Channel-matrix estimation

The 9 received streams described in Section II.-A can be expressed algebraically as functions of time t (with the propagation delays for all channels assumed negligible) by:

$$\vec{y}(t) = \underset{\sim}{H} \times \vec{x}(t) + \vec{n}(t) \tag{1}$$

in which $\boldsymbol{y}(t)$ is a vector representing the 9 streams at time t; $\boldsymbol{x}(t)$ a vector representing values broadcast by the 2 Tx at time t; $\boldsymbol{H}$ a 9-by-2 channel matrix; and $\boldsymbol{n}(t)$ a 9-element vector of random noise.

To estimate the channel matrix $\boldsymbol{H}$ for MIMO demultiplexing, each Tx is enabled in turn, then a sinusoidal training wave $x_j(t)$ with frequency f_j much lower than the bandwidth f_0 of the LED is sent to the enabled Tx and the stream $y_{ij}(t)$ collected from the i^{th} Rx. The element h_{ij} of $\boldsymbol{H}$ corresponding to this particular link is estimated from

$$h_{ij}^2 \cong \frac{\sum_{t=0}^{T} y_{ij}^2(t) - \sigma_i^2 T}{\sum_{t=0}^{T} x_j^2(t)} \tag{2}$$

with T representing the duration of the training wave and σ_i^2 the noise variance corresponding to the i^{th} Rx (estimated from the variance of a pure-noise $y_i(t)$ received when $\boldsymbol{x}(t)$ is all 0.)

B. MIMO Demultiplexing

MIMO demultiplexing is performed by pre-multiplying $\boldsymbol{y}(t)$ with a 2-by-9 matrix $\boldsymbol{G}$ such that $\boldsymbol{z}(t)$ defined as below is considered a good approximation of $\boldsymbol{x}(t)$:

$$\vec{z}(t) = \underset{\sim}{G} \times \vec{y}(t) \tag{3}$$

There are several demultiplexing techniques available. Linear methods include Zero-Forcing and minimum-mean-square-error (MMSE.) Non-linear techniques include the well-known Bell-Labs Layered Space-Time (BLAST) [20] (and its derivative Vertical-BLAST [21])as well as Lattice-Reduction-Aided (LRA) detection [22, 23].

As a compromise between complexity and performance, MMSE demultiplexing is used in our demonstration, with an assumption that the Tx are independent of each other, and have equal average transmission power ρ. The matrix $\boldsymbol{G}$ thus takes the form:

$$\underset{\sim}{G} = \underset{\sim}{H}^{\dagger} \left(\underset{\sim}{H}\underset{\sim}{H}^{\dagger} + \underset{\sim}{C}_N / \rho \right)^{-1} \tag{4}$$

with $\boldsymbol{H}^{\dagger}$ is the Hermitian transpose of $\boldsymbol{H}$; $\boldsymbol{C}_N$ is the ensemble covariance matrix of $\boldsymbol{n}(t)$. The vector $\boldsymbol{z}(t)$ defined in (3) is then passed for subsequent processing.

C. Equalisation

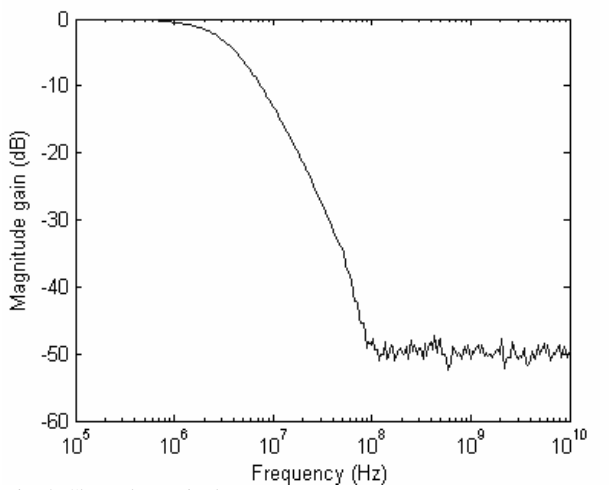

Fig. 4. Channel magnitude response.

The full channel (electrical-optical-electrical) frequency response is shown in Fig. 4, showing the effect of an LED bandwidth of 2MHz and receiver bandwidth of 40MHz. To counter these effects, each of the two MIMO-demultiplexed stream is thus passed through two simple time-domain first-order equalisers [3], with equalisation pole frequency of 2MHz for one and 40MHz for the other.

D. OFDM Demodulation

The demodulation process is achieved by transforming the received waveform into its frequency-domain form using the Fast-Fourier Transform (FFT) operation on a frame-by-frame basis. The 31 active signals are recovered and the constellation quantisation takes place to retrieve the information bits.

IV. Experimental Results

A. Bit-error rate (BER) versus bit-rate

The distance between the Tx and the Rx (R) is set at 100cm. At this distance, the LED spacing is set to s = 6.7cm. This ensures that the images of the Tx at the RX fall in the centre of adjacent pixels.

This spacing is kept constant and the BER vs. bit-rate is measured for R=100cm; a maximum distance of 137cm (larger R would cause both Tx images would fall into a single detector); and a minimum distance of 65cm (smaller R would cause at least one LED to be out of the Rx field of view).

The range of system bit-rates examined is from 60Mbps to 260Mbps. At each bit-rate point, a binary stream of 100,000 bits is tested, with 50,000 bits per channel. If there is no error

in the stream sent, this is represented as $1x10^{-5}$ on the graphs (Fig. 5 and Fig. 6). The system target BER is 10^{-3}, which is acceptable for a forward error correction (FEC) coding algorithm.

Fig. 5 and Fig. 6 show the BER versus the per-channel bit-rate at the three distances for channel 1 and channel 2, respectively. At R = 100cm, each channel can reach a rate of up to 110Mbps before the BER exceeds the target of 10^{-3}. The illuminance at the Rx collection aperture is 800 lux (~400 lux per channel)

At R = 65cm, the upper-bound of the per-channel rate increases to 120Mbps. This is caused by the higher signal-to-noise ratio (SNR) due to higher illuminance at the Rx is measured at 1400 lux (~700 lux per channel) and larger separation between the Tx images which in turn causes the columns of the channel matrix to be more orthogonal, improving the MIMO demultiplexing performance.

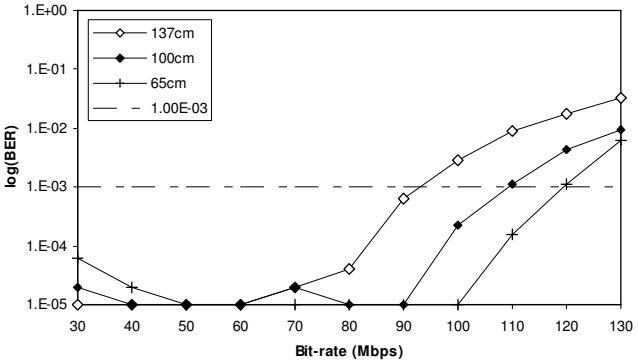

Fig. 5. Bit-error-rate versus bit-rate per channel for channel 1 at the designed distance of 100cm, the maximum distance of 137cm, and the minimum distance of 65cm

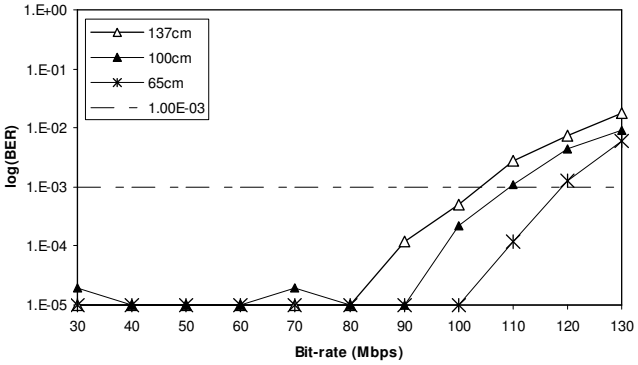

Fig. 6. Bit-error-rate versus bit-rate per channel for channel 2 at the designed distance of 100cm, the maximum distance of 137cm, and the minimum distance of 65cm

At R = 137cm, the illuminance is measured at 320 lux (~150 lux per channel), resulting in lower SNR. For channel 1, the bit-rate that crosses the BER line of 10^{-3} is recorded at 90Mbps (see Fig. 5). At the same distance, the BER curve for channel 2 is better than of channel 1, as a BER of 10^{-3} is achieved at 105Mbps, as shown in Fig. 6. The cause of this difference between the two channels is thought to be of the low SNR received in channel 1, as only half of the LED 1 beam falls on the detector compared with LED 2, where all the images fall on the detector.

B. Coverage area

Coverage is measured at R = 100cm by moving the Tx across the horizontal and vertical directions and measuring the BER whilst the LED spacing s is fixed at 6.7cm.

The coverage area of the system is shown in Fig. 7. The target system BER of 10^{-3} is achieved for 110Mbps/channel within the vertical d_{ver} = 8cm and horizontal d_{hor} = 3cm (where $d_{ver\ and}$ d_{hor} denote the linear coverage in the vertical and horizontal directions). The coverage area is defined as the zone in which images of both the LEDs fall on the receiver, thus allowing MIMO transmission.

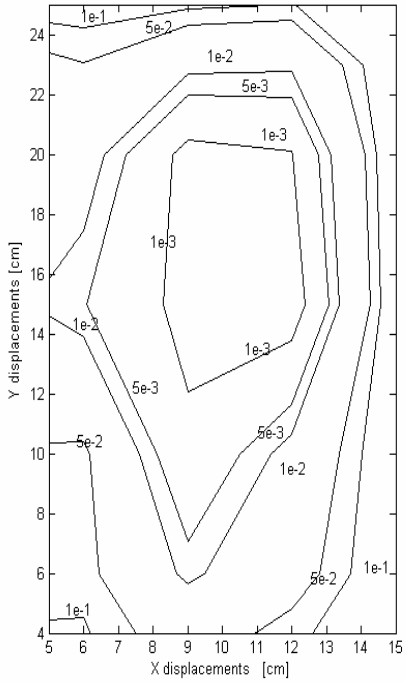

Fig. 7 Coverage area plot at $\boldsymbol{R}$ = 100cm with the contour lines showing the system BER (1e-3 = 1 x 10^{-3}).

Because the variable d_{hor} is measured from the centre of the Tx between the two separated LEDs, the total linear horizontal coverage is therefore $d_{hor} + s$. This is graphically explained by Fig. 8. As a result, the actual linear coverage is 9.7cm horizontal and 8cm vertical, with a beam coverage area of $78cm^2$. Performance degrades away from the centre of the coverage area, due to lower illumination intensity, and falls off rapidly as the source images do not both fall on the receiver.

The measured coverage area is close to that predicted by a geometric optics calculation, with errors likely to be due from estimating the focal length of the receiver lens.

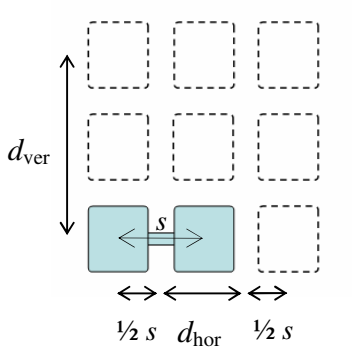

Fig. 8 Total horizontal linear beam coverage diagram.

V. Discussions and Conclusion

This paper presents the design and development of high-speed indoor optical wireless MIMO-OFDM system that uses an imaging receiver. At 100cm range 220Mbps transmission is achieved by combining both channels. The system has a coverage of 8cm x 9.7cm.

The transmission rate is constrained by the low LED bandwidth (~2MHz). Improvements can be made by using an LED with higher bandwidth, equalisation, or by adding a blue filter to block the slow phosphor component at the receiver. A bit-rate of up to 230Mbps/channel has been demonstrated in a single-input single-output (SISO)-OFDM system [24] so there is potential for further improvement.

The high-speed system has a limited coverage area at present. This is limited by the optical power available from the LEDs, as increased coverage requires a greater LED beam divergence. In addition the sources need to be spaced more widely and the receiver optical system redesigned (the system demonstrated in [16] achieves a coverage of ~80x80cm using a greater beam divergence but the much lower level of illumination limits the bit rate to 2Mbps/channel). Further work is required to increase both transmission power and coverage and this is underway.

References

[1]vlcc, "Visible Light Communications Consortium," 2008.

[2]IEEE, " IEEE 802.15.7 WPAN Visual Light Communication Study Group," 2008.

[3]M. Hoa Le, D. O'Brien, G. Faulkner, Z. Lubin, L. Kyungwoo, J. Daekwang, O. YunJe, and W. Eun Tae, "100-Mb/s NRZ Visible Light Communications Using a Postequalized White LED," *Photonics Technology Letters, IEEE,* vol. 21, pp. 1063-1065, 2009.

[4]J. Grubor, S. Randel, K. D. Langer, and J. W. Walewski, "Broadband Information Broadcasting Using LED-Based Interior Lighting," *Lightwave Technology, Journal of,* vol. 26, pp. 3883-3892, 2008.

[5]T. Komine, S. Haruyama, and M. Nakagawa, "Performance evaluation of narrowband OFDM on integrated system of power line communication and visible light wireless communication," *International Symposium on Wireless Pervasive Computing 2006, Conference Program,* pp. 456-461
596, 2006.

[6]M. Z. Afgani, H. Haas, H. Elgala, and D. A. K. D. Knipp, "Visible light communication using OFDM," in *Testbeds and Research Infrastructures for the Development of Networks and Communities, 2006. TRIDENTCOM 2006. 2nd International Conference on*, 2006, p. 6 pp.

[7]G. Yun and M. Kavehrad, "Spot-diffusing and fly-eye receivers for indoor infrared wireless communications," in *Wireless Communications, 1992. Conference Proceedings., 1992 IEEE International Conference on Selected Topics in*, 1992, pp. 262-265.

[8]J. B. Carruthers and J. M. Kahn, "Angle diversity for nondirected wireless infrared communication," *IEEE Transactions on Communications,* vol. 48, pp. 960-969, 2000.

[9]Y. A. Alqudah and M. Kavehrad, "MIMO characterization of indoor wireless optical link using a diffuse-transmission configuration," *IEEE Transactions on Communications,* vol. 51, pp. 1554-60, Sept. 2003.

[10]Garfield-M, Chao-Liang, Kurzweg-Tp, and Dandekar-Kr, "MIMO space-time coding for diffuse optical communication," *Microwave and Optical Technology Letters,* vol. 48, pp. 1108-10, June 2006.

[11]Hranilovic-S and Kschischang-Fr, "Short-range wireless optical communication using pixilated transmitters and imaging receivers," in *2004 IEEE International Conference on Communications. Paris, France. 20 24 June 2004.*, 2004.

[12]Jivkova-S, Hristov-Ba, and Kavehrad-M, "Power-efficient multispot-diffuse multiple-input-multiple-output approach to broad-band optical wireless communications," *IEEE Transactions on Vehicular Technology,* vol. 53, pp. 882-9, May 2004.

[13]D. Takase and T. Ohtsuki, "Optical wireless MIMO communications (OMIMO)," *Globecom '04: Ieee Global Telecommunications Conference, Vols 1-6,* pp. 928-932
4143, 2004.

[14]R. Y. Mesleh, H. Haas, S. Sinanovic, A. Chang Wook, and Y. Sangboh, "Spatial Modulation," *Vehicular Technology, IEEE Transactions on,* vol. 57, pp. 2228-2241, 2008.

[15]A. G. Kirk, "Free-Space Optical Interconnects," in *Optical interconnects : the silicon approach* L. Pavesi and G. G. Guillot, Eds. Berlin: Springer, 2006.

[16]K. D. Dambul, D. O'Brien, and G. Faulkner, "Indoor Optical Wireless MIMO System with an Imaging Receiver," *submitted to Photonics Technology Letters,* 2010.

[17]F. Parand, G. E. Faulkner, and D. C. O'Brien, "Cellular tracked optical wireless demonstration link," *IEE Proceedings Optoelectronics,* vol. 150, pp. 490-6, 17 Oct. 2003.

[18]H. Elgala, R. Mesleh, and H. Haas, "A study of LED nonlinearity effects on optical wireless transmission using OFDM," in *Wireless and Optical Communications Networks, 2009. WOCN '09. IFIP International Conference on*, 2009, pp. 1-5.

[19]H. Elgala, R. Mesleh, and H. Haas, "Practical considerations for indoor wireless optical system implementation using OFDM," in *Telecommunications, 2009. ConTEL 2009. 10th International Conference on*, 2009, pp. 25-29.

[20]G. J. Foschini, "Layered Space-Time architecture for wireless communication in a fading environment when using multi-element antennas,," *Bell Laboratories Technical Journal,* vol. 1, pp. pp. 41-59, Autumn
1996.

[21]P. W. Wolniansky, G. J. Foschini, G. D. Golden, and R. A. Valenzuela, "V-BLAST: an architecture for realizing very high data rates over the rich-scattering wireless channel," in *Signals, Systems, and Electronics, 1998. ISSSE 98. 1998 URSI International Symposium on*, 1998, pp. 295-300.

[22]Y. Huan and G. W. Wornell, "Lattice-reduction-aided detectors for MIMO communication systems," in *Global Telecommunications Conference, 2002. GLOBECOM '02. IEEE*, 2002, pp. 424-428 vol.1.

[23]I. Berenguer, J. Adeane, I. J. Wassell, and W. Xiaodong, "Lattice-reduction-aided receivers for MIMO-OFDM in spatial multiplexing systems," in *Personal, Indoor and Mobile Radio Communications, 2004. PIMRC 2004. 15th IEEE International Symposium on*, 2004, pp. 1517-1521 Vol.2.

[24]J. Vucic, C. Kottke, S. Nerreter, A. Buttner, K. D. Langer, and J. W. Walewski, "White Light Wireless Transmission at 200 + Mb/s Net Data Rate by Use of Discrete-Multitone Modulation," *Photonics Technology Letters, IEEE,* vol. 21, pp. 1511-1513, 2009.